



HAL
open science

Critical Investigation of Heat Transfer Enhancement Using Nanofluids in Microchannels with Slip and Non-Slip Flow Regimes

A. Akbarinia, Morteza Abdolzadeh, R. Laur

► **To cite this version:**

A. Akbarinia, Morteza Abdolzadeh, R. Laur. Critical Investigation of Heat Transfer Enhancement Using Nanofluids in Microchannels with Slip and Non-Slip Flow Regimes. *Applied Thermal Engineering*, 2010, 31 (4), pp.556. 10.1016/j.applthermaleng.2010.10.017 . hal-00699052

HAL Id: hal-00699052

<https://hal.science/hal-00699052>

Submitted on 19 May 2012

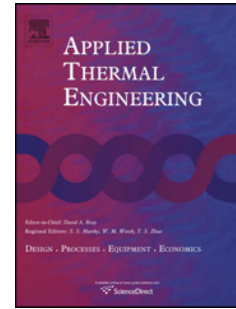
HAL is a multi-disciplinary open access archive for the deposit and dissemination of scientific research documents, whether they are published or not. The documents may come from teaching and research institutions in France or abroad, or from public or private research centers.

L'archive ouverte pluridisciplinaire **HAL**, est destinée au dépôt et à la diffusion de documents scientifiques de niveau recherche, publiés ou non, émanant des établissements d'enseignement et de recherche français ou étrangers, des laboratoires publics ou privés.

Accepted Manuscript

Title: Critical Investigation of Heat Transfer Enhancement Using Nanofluids in Microchannels with Slip and Non-Slip Flow Regimes

Authors: A. Akbarinia, Morteza Abdolzadeh, R. Laur



PII: S1359-4311(10)00444-8

DOI: [10.1016/j.applthermaleng.2010.10.017](https://doi.org/10.1016/j.applthermaleng.2010.10.017)

Reference: ATE 3275

To appear in: *Applied Thermal Engineering*

Received Date: 21 May 2010

Revised Date: 14 October 2010

Accepted Date: 14 October 2010

Please cite this article as: A. Akbarinia, M. Abdolzadeh, R. Laur. Critical Investigation of Heat Transfer Enhancement Using Nanofluids in Microchannels with Slip and Non-Slip Flow Regimes, *Applied Thermal Engineering* (2010), doi: 10.1016/j.applthermaleng.2010.10.017

This is a PDF file of an unedited manuscript that has been accepted for publication. As a service to our customers we are providing this early version of the manuscript. The manuscript will undergo copyediting, typesetting, and review of the resulting proof before it is published in its final form. Please note that during the production process errors may be discovered which could affect the content, and all legal disclaimers that apply to the journal pertain.

Critical Investigation of Heat Transfer Enhancement Using Nanofluids in Microchannels with Slip and Non-Slip Flow Regimes

A. Akbarinia^{a,b*}, Morteza Abdolzadeh^b, R. Laur^a

^a Institute for Electromagnetic Theory and Microelectronics (ITEM), University of Bremen, Germany

^b Department of Mechanical Engineering, Shahid Bahonar University of Kerman, Kerman, Iran

*Corresponding author

Tel: +49 421 21862517

Fax: +49 421 2184434

E-mail: a.akbarinia@item.uni-bremen.de

Abstract:

The Reynolds number in nanofluids studies depends on the inlet velocity and the kinematic viscosity of nanofluid. The nanofluid kinematic viscosity increases with an increasing in nanoparticles volume fraction while the inlet velocity should be increased to keep the Reynolds number constant. Therefore, it is not clear that either increasing the nanoparticles volume fraction or increasing the inlet velocity has major role on heat transfer enhancement in nanofluids flow studies which are done at constant Reynolds numbers. In this study, forced convection Al_2O_3 -water nanofluid flows in two-dimensional rectangular microchannels have been investigated to study heat transfer enhancement due to addition of the nanoparticles to the base fluid especially in microchannels at low Reynolds number. Three

different cases are examined to evaluate proportion impact of increasing nanoparticles volume fraction (ϕ) and the inlet velocity (u_{in}) on heat transfer enhancement. Two-dimensional Navier-Stokes and energy equations accompany with the slip velocity and the jump temperature boundary conditions expressions have been discretized using the Finite Volume Method (*FVM*). The Brownian motions of nanoparticles have been considered to determine the thermal conductivity of nanofluids. The calculated results show good agreement with the previous numerical and analytical data. It is found that at a given Reynolds number, the major enhancement in the Nusselt number is not due to increasing the nanoparticle concentrations but it is due to the increasing the inlet velocity to reach a constant Re . Constant Reynolds number studies of nanofluids are not sufficient approach to evaluate the heat transfer and the skin friction factor due to the nanofluids usage.

Keywords: Nanofluid, Microfluidic, Heat transfer, Slip flow, Rarefaction, Microchannel.

Nomenclature

C_p	specific heat ($\text{kJ kg}^{-1} \text{K}^{-1}$)
d	diameter of nanoparticle or water molecular
D_h	hydraulic diameter (m)
f	Fanning friction coefficient, $(= \frac{\tau_w}{\left(\frac{1}{2} \rho_{nf} \bar{u}^2\right)})$
h	heat transfer coefficient ($\text{Wm}^{-2}\text{K}^{-1}$)
k	thermal conductivity ($\text{Wm}^{-1} \text{K}^{-1}$)
k_B	Boltzmann constant ($=1.3807 \times 10^{-23} \text{ j/k}$)
Kn	Knudsen number (λ/D_h)

- L length of microchannel (m)
- Nu_x local Nusselt number, $(= \frac{h_x D_h}{k_{nf}})$
- q'' heat flux at the wall
- p pressure (Pa)
- P non-dimensional pressure
- Po Poiseuille number, $(= \frac{\tau_w D_h}{\left(\frac{1}{2} \mu_{nf} \bar{u}\right)})$
- Pe_{nf} Peclet number $(= Re_{nf} Pr_{nf})$
- Pr_{nf} Prandtl number $(= \frac{\mu_{nf} (C_p)_{nf}}{k_{nf}})$
- Re_{nf} Reynolds number $(= \frac{\rho_{nf} u_{in} D_h}{\mu_{nf}})$
- T temperature
- u velocity ($m s^{-1}$)
- U non-dimensional velocity
- W width of microchannel (m)
- x, y coordinates
- X, Y non-dimensional coordinates
- X^* reciprocal Graetz number $(x/(D_h Pe))$

Greek letters

- α thermal diffusivity $(= \frac{k}{\rho C_p})$
- β variable, defined in Eq. (19)
- γ specific heat ratio $(= \frac{C_p}{C_v})$

θ	non-dimensional temperature ($= \frac{T - T_{in}}{T_{wall} - T_{in}}$)
λ	mean free path (m)
η	variable, defined in Eq. (14)
μ	dynamic viscosity (N s m^{-2})
ρ	density (kg m^{-3})
σ_T	thermal accommodation coefficient
σ_v	momentum accommodation coefficient
τ_w	shear stress at the wall, ($= -\mu_{nf} \left. \frac{\partial u}{\partial y} \right _{wall}$)
ν	kinematic viscosity ($\nu_{nf} = \mu_{nf} / \rho_{nf}$)
ϕ	nanoparticles volume fraction
Φ	independent variable

Subscripts

b	balk
en	entrance length
f	base fluid
fd	fully developed
i, j	array indices
in	inlet condition
N	closed to the wall
nf	nanofluid
s	solid nanoparticles
wall	at the wall

1. Introduction

With the development of science and technology, people begin to realize that with the size decreasing the system will own many advantages that do not appear in conventional size, including compact size, disposability, and increased functionality [1]. Microchannels, however, are the basic structures in these systems. Based on the Knudsen number (Kn), the flow in microchannels have been classified into four flow regimes: continuum flow regime ($Kn \leq 0.001$), slip flow regime ($0.001 < Kn \leq 0.1$), transition flow regime ($0.1 < Kn \leq 10$) and free molecular flow regime ($Kn > 10$). The flow in most application of these systems, such as Micro Gyroscope, Accelerometer, Flow Sensors, Micro Nozzles, Micro Valves, is in slip flow regime, which is characterized by slip flow at wall. Traditionally, the no-slip condition at wall is enforced in the momentum equations and an analogous no-temperature-jump condition is applied in the energy equation. Strictly speaking, no-slip/no-jump boundary conditions are valid only if the fluid flow adjacent to the surface is in thermodynamic equilibrium. This requires an infinitely high frequency of collisions between the fluid and the solid surface [1,2]. In practice, the no-slip/no-jump condition leads to fairly accurate predictions as long as $Kn < 0.001$. Beyond that, flow in devices shows significant slip since characteristic length is on the order of the mean free path of the fluid or gas molecules. It means that the collision frequency is simply not high enough to ensure equilibrium and a certain degree of tangential velocity slip and temperature jump must be appeared. Slip velocity at the wall is the most important feature in micro/nano scale that differs from conventional internal flow. Therefore, the slip flow characteristics are very important for designing and optimizing the micro/nano systems. On the other hand, the optimization of microchannels design is affected significantly by their reliability and thermal performance. It is found that the temperature jump effects are very important and should be included in the modeling of the slip flow heat transfer problems, and neglecting these effects leads to a significant overestimate of heat transfer coefficient [3, 4].

In most of the previous research, low thermal conductivity base fluids such as air or water have been employed to study the fluid flow in microchannel. The heat transfer of fluids flow is limited base on thermal properties of fluids. However, demanding for increasing the heat transfer in microchannel needs to improve thermal properties of base fluids. One of the presented solutions for this problem is adding solid nanoparticles with high thermal conductivity such as Al_2O_3 , Cu or CuO to the base fluid which are called nanofluids. During the past two decades, scientists and researchers have been attempting to develop nanofluids, which can offer better heating and cooling performance for variety of thermal systems compared to traditional heat transfer fluids. It is found by numerous numerical and experimental studies that the nanofluids have high thermal conductivities and abilities to increase the heat transfer [5, 6, 7, 8]. The major attempts have been done to investigate the effective thermal conductivity of nanofluids and the effective dynamic viscosity for predicting the thermal conductivity and dynamic viscosity of nanofluids [9]. The most of papers have reported an enhancement in the heat transfer due to increasing the nanoparticle concentration which are done at constant Reynolds number. But some researchers have reported an uncertainty in heat transfer enhancement of nanofluids flow [10, 11]. Akbarinia [10] have investigated heat transfer in the nanofluids flow with constant mass flow rate and reported a reducing in heat transfer with increasing nanoparticles volume fraction.

Recently, the nanofluids utilization in microchannel has been received a great interest amongst researchers. Koo and Kleinstreuer[12], Jang and Choi[13] and Chein and Huang [14] have studied experimentally improving thermal performance of the nanofluids flow in microchannel with different nanofluid such as CuO -water or Al_2O_3 -water. The thermal performance of microchannels using nanofluids base on different models for effective thermal conductivity also has been investigated numerically by [15-20]. They have evaluated the impacts of parameters such as microchannel geometry, Reynolds number and nanoparticles volume fraction on the thermal performance of nanofluid flow in microchannels. They have

reported higher heat transfer performance of nanofluids flow compare to the base fluids in microchannels at constant Reynolds number. However, all of them have used the non-slip flow regimes in their numerical research works.

To the best knowledge of the authors, the major of previous numerical and experimental studies on nanofluids flow and heat transfer have been done with constant Reynolds number. The Reynolds number in nanofluids studies depend on the inlet velocity and the kinematic viscosity of nanofluid. The nanofluid kinematic viscosity increases with an increasing in nanoparticles volume fraction while the inlet velocity should be increased to keep the Reynolds number constant. Therefore, it is not clear that either increasing the nanoparticles volume fraction or increasing the inlet velocity has major role on heat transfer enhancement in nanofluids studies which are done at constant Reynolds numbers.

The objective of the present paper is to study the proportion impact of nanoparticle volume fraction (ϕ) and the inlet velocity (u_{in}) on heat transfer of nanofluids flow at constant Reynolds numbers especially in microchannels with low Reynolds numbers and answer to this question “ Does the nanofluid increase heat transfer?”. To aim to this purpose, laminar forced convection slip and non-slip Al_2O_3 -water nanofluid flow in a rectangular microchannel have been investigated, employing the slip velocity and the jump temperature boundary conditions at the fluid-wall interface. Three different cases are examined to evaluate proportion impact of increasing nanoparticles volume fraction (ϕ) and the inlet velocity (u_{in}) on heat transfer enhancement. Simultaneous effects of the inlet velocity and the nanoparticles volume fraction on heat transfer augmentation are studied. The axial velocity, Poiseuille number, temperature and Nusselt number profiles are presented and discussed. Although the study is done in a microchannel with slip flow regimes, but results are also presented for the case no-slip flow ($Kn=0$) which could cover for the macro scale.

2. Analysis

2.1 Governing equations

The schematic of the channel and coordinate system are shown in Fig. 1. The flow is considered along the x-axis and the channel length is chosen 20 time width in order to achieve hydrodynamically developed flow at the outlet.

The Al_2O_3 -water nanofluid flow and the heat transfer in rectangular microchannels have been considered. The nanofluid flow is laminar, steady state and incompressible with constant properties while dissipation, pressure work and body forces are neglected. The used properties of base fluid (water) and solid nanoparticles (Al_2O_3) are presented in Table 1. The rarefaction effects set the slip velocity and the jump temperature at the fluid–wall interface. Therefore, the steady state governing equations describing the fluid flow and the heat transfer in the microchannel in the Cartesian coordinate and in the tensors form are as follows:

Continuity equation:

$$\frac{\partial u_j}{\partial x_j} = 0 \quad (1)$$

Momentum equations:

$$\rho_{nf} \frac{\partial}{\partial x_j} (u_i u_j) = \mu_{nf} \frac{\partial}{\partial x_j} \left(\frac{\partial u_i}{\partial x_j} \right) - \frac{\partial p}{\partial x_i} \quad (2)$$

Fluid energy equation:

$$(\rho C_p)_{nf} \frac{\partial}{\partial x_i} (u_i T) = k_{nf} \frac{\partial}{\partial x_i} \left(\frac{\partial T}{\partial x_i} \right) \quad (3)$$

Where $i=1, 2$ and $u_i=(u_x, u_y)$ are velocity vectors.

The continuity, momentum and fluid energy equations are non-dimensionalized using following dimensionless parameters:

$$X_i = \frac{x_i}{D_h}, U_i = \frac{u_i}{u_{in}}, P = \frac{p}{\rho_{nf} u_{in}^2} \text{ and } \theta = \frac{T - T_{in}}{T_{wall} - T_{in}} \quad (4)$$

Where $D_h \approx 2W$.

Therefore, the non-dimensionalized governing equation becomes as follow:

Continuity equation:

$$\frac{\partial U_j}{\partial X_j} = 0 \quad (5)$$

Momentum equations:

$$\frac{\partial}{\partial X_j} (U_i U_j) = \frac{1}{Re_{nf}} \left(\frac{\partial^2 U_i}{\partial X_j^2} \right) - \frac{\partial P}{\partial X_i} \quad (6)$$

Fluid energy equation:

$$\frac{\partial}{\partial X_i} (U_i \theta) = \frac{1}{Pe_{nf}} \frac{\partial^2 \theta}{\partial X_i^2} \quad (7)$$

Where $Pe_{nf} = Re_{nf} Pr_{nf}$, $Re_{nf} = \frac{\rho_{nf} u_{in} D_h}{\mu_{nf}}$ and $Pr_{nf} = \frac{\mu_{nf} (C_p)_{nf}}{k_{nf}}$ are the Peclet number, the

Reynolds number and the Prandtl number, respectively.

2.2 Nanofluid properties

The physical properties of nanofluid containing water- Al_2O_3 can be calculated as follow:

Density:

$$\rho_{nf} = (1 - \phi) \rho_f + \phi \rho_s \quad (8)$$

Heat capacitance:

$$(\rho C_p)_{nf} = (1 - \phi) (\rho C_p)_f + \phi (\rho C_p)_s \quad (9)$$

The presented expression for dynamic viscosity by Maiga et al. [21] which was determined based on available experimental results for water- Al_2O_3 is given as:

$$\mu_{nf} = (123\phi^2 + 7.3\phi + 1) \mu_f \quad (10)$$

The thermal conductivity of water- Al_2O_3 nanofluid has been determined from Chon et al. [22] correlation which considers the Brownian motion and mean diameter of the nanoparticles as follow:

$$\frac{k_{nf}}{k_f} = 1 + 64.7 \phi^{0.7460} \left(\frac{d_f}{d_s}\right)^{0.3690} \left(\frac{k_s}{k_f}\right)^{0.7476} Pr_f^{0.9955} Re_f^{1.2321} \quad (11)$$

Where Pr_f and Re_f in Eq.(11) are defined as:

$$Pr_f = \frac{\mu}{\rho_f \alpha_f} \quad (12)$$

$$Re_f = \frac{\rho k_B T}{3\pi \eta^2 \lambda_f} \quad (13)$$

Where λ_f is mean free path of water molecular ($\lambda_f = 0.17\text{nm}$), k_B is Boltzmann constant ($k_B = 1.3807 \times 10^{-23} \text{ j/k}$) and η has been calculated by the following equation:

$$\eta = A \cdot 10^{\frac{B}{T-C}}, \quad A = 2.414 \times 10^{-5}, \quad B = 247.8, \quad C = 140 \quad (14)$$

2.3 Slip velocity and jump temperature

The second order non-dimensionalized velocity slip condition is expressed as [23]:

$$U = \left(\frac{2 - \sigma_v}{\sigma_v}\right) Kn \frac{\partial U}{\partial Y} \Big|_{wall} + \frac{3}{2\pi} \frac{(\gamma - 1) Kn^2 Re}{\gamma Ec} \frac{\partial \theta}{\partial X} \Big|_{wall} \quad (15)$$

Here Ec is Eckert number ($Ec = \frac{U^2}{C_p \Delta T}$). The second term can be negligible if $\frac{\partial}{\partial Y} \gg \frac{\partial}{\partial X}$ at

the wall and also due to fact that it is second order in the Knudsen number. Similar arguments can be applied to the jump temperature boundary condition, and the resulting from Taylor series leads in dimensionless form [23]:

$$\theta - \theta_{wall} = \left(\frac{2 - \sigma_T}{\sigma_T}\right) \left(\frac{2\gamma}{\gamma + 1}\right) \frac{1}{Pr} \left[Kn \left(\frac{\partial \theta}{\partial Y} \Big|_{wall}\right) + \frac{Kn^2}{2!} \left(\frac{\partial^2 \theta}{\partial Y^2} \Big|_{wall}\right) + \dots \right] \quad (16)$$

Values of the thermal and momentum accommodation coefficients (σ_v, σ_T) are near unity for

most engineering applications and they are taken as unity in the present study.

After simplifying, the non-dimensional forms of the slip flow velocity and jump temperature boundary conditions are given by:

$$U_N - U_{wall} = Kn \frac{\partial U}{\partial Y} \Big|_{wall} \quad (17)$$

$$\theta_N - \theta_{wall} = \frac{Kn}{\beta} \frac{\partial \theta}{\partial Y} \Big|_{wall} \quad (18)$$

Where

$$\beta = \text{Pr} \left(\frac{\gamma + 1}{2\gamma} \right), \quad (19)$$

$$\theta_{wall}=1 \text{ and } U_{wall}=0$$

2.4 Boundary conditions

These set of nonlinear elliptical governing equations have been solved subject to following boundary conditions:

- At the channel inlet: the nanofluid velocity and the temperature profiles are assumed uniform and constant ($X=0, 0 \leq Y \leq 0.5: U=1, \theta=0$).
- At the fluid-solid interface: The velocity in y direction is zero while the slip velocity and the jump temperature of the nanofluid flow adjacent to the wall is proportional to normal velocity and the temperature gradients at the fluid-wall interface (Equations (17) and (18)). A constant temperature ($\theta_{wall}=1$) at the wall is also applied.
- At the channel outlet: the diffusion flux in the direction normal to the exit is assumed to be zero for the velocity and the temperature while a zero pressure is assigned at the flow exit.

$$(X=10, 0 \leq Y \leq 0.5: \frac{\partial U}{\partial X} = \frac{\partial \theta}{\partial X} = 0, P=0)$$

3. Numerical methods and validations

The sets of coupled non-linear differential equations were discretized using the Finite Volume Method (*FVM*). The power law scheme was used for the convective and diffusive terms while the *SIMPLER* procedure was introduced to couple the velocity-pressure as described by Patankar [24]. The slip velocity and the jump temperature boundary conditions expressions are discretized and employed in the discretization equations.

A structured non uniform grid distribution has been used for the computational domain. It is finer near the microchannel entrance and near the wall where the velocity and the temperature gradients are high. Channel lengths are set to a value greater than the estimated entrance lengths to ensure that fully developed conditions are achieved at the exit. Several different grid distributions have been tested to ensure that the calculated results are grid independent. As it is shown in Fig.2 increasing the quantity of nodes more than 60 nodes in y direction and 160 nodes in x direction do not change the velocity significantly. Therefore, the selected grid for the present calculations consisted of 160×60 nodes in the x and y directions respectively.

The solution is assumed converged when $\left| \frac{(\Phi^{n+1} - \Phi^n)}{\Phi^{n+1}} \right| \leq 10^{-6}$ is satisfied for all independent variables.

After solving the governing equations for velocity, pressure and temperature other useful quantities such as Nusselt number and Poiseuille number can be determined.

The local Poiseuille number (fRe_x) can be obtained by:

$$f Re_x = 2 \frac{\left. \frac{\partial u}{\partial y} \right|_{wall}}{\bar{u}} D_h \quad (20)$$

After using dimensionless parameters, it becomes as follow:

$$f Re_x = 2 \left. \frac{\partial U}{\partial Y} \right|_{wall} \quad (21)$$

By submitting the term $\left. \frac{\partial U}{\partial Y} \right|_{wall}$ from Eq.(17) into Eq.(21), the local Poiseuille number for the

slip flow regimes can be expressed as:

$$f \text{Re}_x = \frac{2}{Kn} U_N \quad (22)$$

The local Nusselt number (Nu_x) can be obtained by:

$$\text{Nu}_x = \frac{h_x D_h}{k} \quad (23)$$

Where:

$$h_x = \frac{q''}{(T_{wall} - T_b)} \quad \text{and} \quad q'' = -k \left. \frac{\partial T}{\partial y} \right|_{wall} \quad (24)$$

After normalizing and combination of Eq.(23) and Eq.(24), the local Nusselt number for the case of uniform wall temperature can be calculated from:

$$\text{Nu}_x = \frac{\left. \frac{\partial \theta}{\partial Y} \right|_{wall}}{\theta_b - \theta_{wall}} \quad (25)$$

Where the bulk temperature can be calculated from:

$$\theta_b(X) = \frac{\int_0^{L/D_h} \theta(X, Y) U(X, Y) dY dX}{\int_0^{W/D_h} U(X, Y) dY dX} \quad (26)$$

By substituting the term $\left. \frac{\partial \theta}{\partial Y} \right|_{wall}$ from Eq. (18) into Eq. (25), the local Nusselt number for

the slip flow regimes can be expressed as:

$$\text{Nu}_x = \frac{\frac{\beta}{Kn} (\theta - \theta_{wall})}{\theta_b - \theta_{wall}} \quad (27)$$

In order to demonstrate the validity and also precision of the model assumptions and the numerical analysis, fully developed values of the Poiseuille numbers are compared with available numerical and analytical solutions at $Re=100$ for different Kn . The calculated

Poiseuille numbers in Fig.3 show a good agreement with numerical results by M.Renksizbulut

et al. [25] and analytical values, which vary with Kn according to $f Re_{fd} = \frac{24}{(1+12Kn)}$. The

local Nusselt numbers are presented in Fig.4 and are compared also with the results by Yu and Ameer [26] for $Kn=0.04$, $\beta=10$ and infinity aspect ratio. As seen from this figure a significant agreement between the calculated and numerical results are observed.

4. Results and discussion

Numerical simulations have been done for three different cases to evaluate the impact of the Al_2O_3 nanoparticle volume fraction and the inlet velocity on heat transfer enhancement in the non-slip and slip nanofluid flow regimes. The first case (I) is done with a constant Reynolds number where the inlet velocity increases with increasing ϕ in order to keep Re constant. The second case (II) is done for the pure fluid ($\phi=0$) where only the inlet velocity increases according to the used inlet velocity in the first case (I) for different ϕ . The third case (III) is done with a constant inlet velocity ($u_{in}=0.0502$ m/s according to the used inlet velocity for $\phi=0$ in the first case (I)) where only the nanoparticles volume fraction increases without keeping Re constant.

Hence the major fluid flows in the microchannels are laminar flow with low Reynolds numbers, for this study low Reynolds numbers ($7 \leq Re \leq 15$) are chosen. The non-slip and slip flow simulations for these three cases have been also presented. The nanoparticles volume fraction varies from 0 to 5%, because most published paper have also done in this range. The used values for the inlet velocity and other calculated values of two ϕ ($\phi=0$ and $\phi=5\%$) for the first case (I), the second case (II) and the third case (III) are presented in Table 2, Table 3 and Table 4, respectively.

4.1. Velocity field

The velocity profiles for different nanoparticles volume fraction (ϕ) at $Re=10$ and $Kn=0.01$ are shown in Fig. 5. The non-dimensional momentum equation (Eq.(6)) is only depend on the Reynolds number. Therefore, at a given Re the solid volume fraction does not have any effect on the non-dimensional velocity which is illustrated in Fig. 5a and 5b. However at a given Re , the inlet velocity should be increased with increasing the solid volume fraction to keep Re constant. Consequently, the velocity in any cross section increase which is presented in Fig.5c and 5d. As it is shown in Table 2, the kinematic viscosity ($\nu_{nf} = \mu_{nf}/\rho_{nf}$) of nanofluid increases with increasing the nanoparticle volume fraction in a given Re , therefore the inlet velocity should be increased. In the previous works which are done with constant Reynolds numbers, it is not clear that the reported effects of nanofluid on heat transfer and friction factor are due to either the adding the solid nanoparticles to the base fluid or increasing the inlet velocity.

4.2. Skin friction factor

The local Poiseuille number at different ϕ , Kn and Re is presented in Fig.6 for the first case (I) and second case (II). The nanoparticle volume fraction does not have any effect on the non-dimensional velocity at a given Re (see Fig.5a and 5b). Consequently, it does not have any effect on the Poiseuille number in the micro or macro ($Kn=0$) scale for the first case (I) as depicted in Fig.6a and 6b, respectively. The Fig. 6c and 6d show that for the second case (II) because of small variation in the Reynolds numbers, fRe does not change significantly when the nanoparticles volume fraction increases.

4.3. Temperature field

The non-dimensional temperature and non-dimensional bulk temperature for three cases are presented in Fig. 7. Increasing ϕ for the first case (I) decreases the temperature and bulk

temperature at any cross section at a given Re . Is the reduction due to either increasing the nanoparticles volume fraction or increasing the inlet velocity?

Figures of second case (II) show that increasing inlet velocity also reduces the temperature and the bulk temperature at any cross section like the first case (I). But increasing the nanoparticles volume fraction without increasing the inlet velocity does not have any significant effect on the temperature which is illustrated in Fig. 7 third row (third case (III)).

4.4. Nusselt number

Variations of the local Nusselt number in three cases are shown in Fig.8. As it is reported by previous researcher, increasing the nanoparticles volume fraction increases the local Nusselt number in the non-slip and slip flow regimes for the first case (I) at a given Re . For the second case (II), increasing the inlet velocity also increases the local Nusselt number as well as increasing ϕ for the first case (I).

With considering the third case (III) in Fig.7, Fig.8 and Table3 it is obvious that adding solid volume nanoparticles to the base fluid increases the thermal conductivity and Prandtl number while the Reynolds number reduces. As a result, the Peclet number does not change significantly when the solid nanoparticles volume fraction increases. Consequently, increasing ϕ without increasing the inlet velocity does not have any significant effect on the local Nusselt number at the third case (III). This behavior also have been observed by Santra et al. [27] at low Reynolds number ($Re < 100$) in which the Copper (with very high thermal conductivity $K_s = 386$) nanoparticles volume fraction does not have any notable effect on the average Nusselt number (Fig.7 in [27]) in isothermally heated parallel plates.

5. Conclusions

The Reynolds number in nanofluids studies depends on the inlet velocity and kinematic viscosity of nanofluid. The nanofluid kinematic viscosity increases with an increasing in nanoparticles volume fraction while the inlet velocity should be increased to keep the Reynolds number constant. Therefore, it is not clear that either increasing the nanoparticles volume fraction or increasing the inlet velocity has major role on heat transfer enhancement in nanofluids studies which are done at constant Reynolds numbers.

Forced convection Al_2O_3 -water nanofluid flows in two-dimensional rectangular microchannels have been investigated to study heat transfer enhancement due to application of the nanoparticles to the base fluid. Three different cases are examined to evaluate the proportion impact of increasing the nanoparticles volume fraction (ϕ) and the inlet velocity (u_{in}) on heat transfer enhancement. Two-dimensional Navier-Stokes and energy equations accompany with the slip velocity and the jump temperature boundary conditions expressions have been discretized using the finite volume technique. The Brownian motions of nanoparticles have been considered to determine the thermal conductivity of nanofluids. The following conclusions are obtained:

- Results clearly show that at a given Reynolds number (Re), the non-dimensional velocity is not affected by the volume fraction of nanoparticles but the inlet velocity should be increased to keep Re constant.
- The nanoparticles concentration has not any notable effect on the Poiseuille number (fRe) at any Re .
- At a given Reynolds number, the temperature decreasing is not due to increasing the nanoparticles concentration, but it is due to increasing the inlet velocity.
- It is shown that at a given Re , the major enhancement in the Nusselt number is not due to increasing the nanoparticle concentrations but it is due to the increasing the inlet velocity to reach a constant Re . Increasing the nanoparticle concentration does

not change the Peclet number significantly, therefore it does not have any significant effect on the heat transfer at a constant inlet velocity.

- Increasing the nanoparticles volume fraction increases density and dynamics viscosity which could increase pumping power. On the other hand, increasing inlet velocity increases pumping power at a given Re . It has been shown that the same heat transfer enhancement could be reached only with the same increasing in inlet velocity without employing nanofluids.
- Constant Reynolds number studies of nanofluids are not sufficient to evaluate the heat transfer and the skin friction factor due to the nanofluids usage.

Further numerical and experimental investigations are needed to develop an appropriate method such as constant pumping powers for investigation heat transfer due to the nanofluids application where could clearly answer to this question “Is nanofluids application useful and economic?”

6. References

- [1] M. Gad-el-Hak, The Fluid Mechanics of Microdevices: The Freeman Scholar Lecture, *J. Fluids Eng.* 121 (1999), 5–33.
- [2] A. Beskok, G.E. Karniadakis, Simulation of Heat and Momentum Transfer in Complex Micro-Geometries, *J. Thermophys. Heat Transfer* 8 (4) (1994) 355-370.
- [3] F.E. Larrodé, C. Housiadas, Y. Drossinos, Slip-flow heat transfer in circular tubes, *Int. J. Heat Mass Transf.* 43 (2000) 2669–2680.
- [4] W. Sun, S. Kakac, A.G. Yazicioglu, A numerical study of single-phase convective heat transfer in microtubes for slip flow, *Int. J. Therm. Sci.* 46 (2007) 1084–1094.
- [5] B.C. Pak and Y.I. Cho, Hydrodynamic and heat transfer study of dispersed fluids with submicron metallic oxide particles, *Exp. Heat Transfer* 11 (1998), pp. 151–170.

- [6] Y.M. Xuan and Q. Li, Investigation on convective heat transfer and flow features of nanofluids, *J. Heat Transfer* 125 (2003), pp. 151–155.
- [7] A. Akbarinia, A. Behzadmehr, Numerical Study of Laminar Mixed Convection of a Nanofluid in Horizontal Curved Tubes, *Applied Thermal Eng.*, 27 (8-9), (2007), 1327-1337.
- [8] A. Akbarinia, R. Laur, Investigation the Diameter of solid Particles affects on a Laminar Nanofluid Flow in a Curved Tube Using a Two Phase Approach, *Int. J. Heat fluid flow*, 30 (4), (2009) 706-714.
- [9] S.M.S. Murshed, K.C. Leong , C. Yang, Thermophysical and electrokinetic properties of nanofluids – A critical review, *Applied Thermal Engineering*, 28 (2008) 2109–2125.
- [10] A. Akbarinia, Impacts of Nanofluid Flow on Skin Friction Factor and Nusselt Number in Curved Tubes with Constant Mass flow, *Int. J. Heat Fluid Flow*, 29 (1), (2008) 229-241.
- [11] C.T. Nguyen, F. Desgranges, N. Galanis, G. Roy, T. Maré, S. Boucher, H. Angue Mintsu, Viscosity data for Al_2O_3 –water nanofluid—hysteresis: is heat transfer enhancement using nanofluids reliable?, *Int. J. of Thermal Sciences*, 47 (2008) 103–111.
- [12] J. Koo, C. Kleinstreuer, Laminar nanofluid flow in microheat-sinks, *International Journal of Heat and Mass Transfer*, 48 (13) (2005) 2652-2661.
- [13] S.P. Jang, S.U.S. Choi, Cooling performance of a microchannel heat sink with nanofluids, *Applied Thermal Engineering*, 26 (17-18) (2006) 2457-2463.
- [14] R. Chein, G. Huang, Analysis of microchannel heat sink performance using nanofluids, *Applied Thermal Engineering*, 25 (17-18) (2005) 3104-3114.
- [15] H. Abbassi, C. Aghanajafi, Evaluation of heat transfer augmentation in a nanofluid-cooled microchannel heat sink, *Journal of Fusion Energy*, 25 (3-4) (2006) 187-196.
- [16] T.H. Tsai, R. Chein, Performance analysis of nanofluid-cooled microchannel heat sinks, *International Journal of Heat and Fluid Flow*, 28 (5) (2007) 1013-1026.
- [17] J. Li, C. Kleinstreuer, Thermal performance of nanofluid flow in microchannels, *International Journal of Heat and Fluid Flow*, 29 (4) (2008) 1221-1232.

- [18] R. Chein, J. Chuang, Experimental microchannel heat sink performance studies using nanofluids, *International Journal of Thermal Sciences*, 46 (1) (2007) 57-66.
- [19] J.Y. Jung, H.S. Oh, H.Y. Kwak, Forced convective heat transfer of nanofluids in microchannels, *International Journal of Heat and Mass Transfer*, 52 (1-2) (2009) 466-472.
- [20] C.J. Ho, L.C. Wei, Z.W. Li, An experimental investigation of forced convective cooling performance of a microchannel heat sink with Al₂O₃-water nanofluid, *Applied Thermal Engineering*, 30 (2-3) (2010) 96-103.
- [21] S.E.B. Maiga, C.T. Nguyen, N. Galanis and G. Roy, Heat transfer behaviors of nanofluids in a uniformly heated tube, *Superlatt. Microstruct.* 35 (2004), pp. 543–557.
- [22] C.H. Chon, K.D. Kihm, S.P. Lee, S.U.S. Choi, Empirical correlation finding the role of temperature and particle size for nanofluid (Al₂O₃) thermal conductivity enhancement, *Appl. Phys. Lett.* 87 (2005) 1–3.
- [23] Mohamed Gad-el-Hak, *The MEMS Handbook, MEMS: Introduction and Fundamentals*, Second Edition, Taylor & Francis Group, 2006.
- [24] S.V. Patankar, *Numerical Heat Transfer and Fluid Flow*, Hemisphere, Washington, 1980.
- [25] M. Renksizbulut, H. Niazmand, G. Tercan, Slip-flow and heat transfer in rectangular microchannels with constant wall temperature, *Int. J. Therm. Sci.* 45 (9) (2006) 870–881.
- [26] S. Yu, T.A. Ameel, Slip flow heat transfer in rectangular microchannels, *Int. J. Heat Mass Transf.* 44 (2001) 4225–4234.
- [27] A.K. Santra, S. Sen, N. Chakraborty, Study of heat transfer due to laminar flow of copper-water nanofluid through two isothermally heated parallel plates, *Int. J. Thermal Sciences*, 48 (2) (2009) 391-400.

List of Table

Table 1. Thermophysical Properties of nanoparticles and base fluid at 27⁰C.

Table 2. Calculated values for the first case (I) at a constant Reynolds number.

Table 3. Calculated values for the second case (II) at $\phi=0$ and the corresponding inlet velocity values in the first case (I).

Table 4. Calculated values for the third case (III) at a constant inlet velocity and different ϕ .

List of Figures

Figure1. Schematic diagram of two-dimension rectangular microchannel.

Figure.2 Grid independent test a) in x direction b) in y direction.

Figure.3 Compare the fully developed Poiseuille number with the previous numerical results by Renksizbulut et al. [25] and also with analytical results.

Figure.4 Compare the local Nusselt number with the previous numerical results by Yu and Ameen [26] for $Kn=0.04$ and $\beta=10$ with infinity aspect ratio.

Figure.5 Variation of the non-dimensional velocity (a,b) and dimensional velocity profile (c,d) with nanoparticles concentration for $Re=10$ and $Kn=0.01$ at fully developed region a) and c), at centerline along the channel b) and d).

Figure.6 The local Poiseuille number profiles for first case (I) and second case (II) at $Re=10$ and different ϕ for a) slip flow regime ($Kn=0.01$) and b) non-slip flow regimes ($Kn=0$).

Figure.7 a) the non-dimensional temperature at the outlet and b) the non-dimensional bulk temperature profiles for first case (I), second case (II) and third case (III).

Figure.8 The local Nusselt number profiles for first case (I), second case (II) and third case (III) for a) slip flow regime ($Kn=0.01$) and b) non-slip flow regimes ($Kn=0$).

Table 1.

Thermophysical Properties of nanoparticles and base fluid at 27°C

Properties	Water	Nanoparticle(Al_2O_3)
Density ρ (kg/m^3)	998.2	3890
Heat capacitance C_p (J/kg.K)	4240	880
Thermal conductivity k (W/mK)	0.608	35

Table 2.

Calculated values for the first case (I) at a constant Reynolds number.

Re	ϕ	u_{in}	μ_{nf}/ρ_{nf}	C_p	k_{nf}	Pr	Pe
10	0	0.0502	1.0048e-006	4242	0.608	7	70
10	5%	0.0734	1.4679e-006	4203	0.687	10.3	103

Table 3.

Calculated values for the second case (II) at $\phi=0$ and the corresponding inlet velocity values in the first case (I).

u_{in}	ϕ	Re	Pr	Pe
0.0502	0	10	7	70
0.0734	0	14.6	7	102.2

Table 4.

Calculated values for the third case (III) at a constant inlet velocity and different ϕ .

ϕ	u_{in}	μ_{nf}/ρ_{nf}	C_p	k_{nf}	Re	Pr	Pe
0	0.0502	1.0048e-006	4242	0.608	10	7	70
5%	0.0502	1.4679e-006	4203	0.687	6.9	10.3	71.1

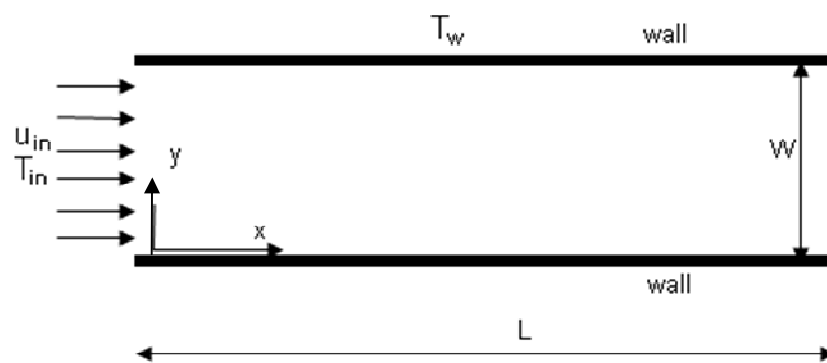


Fig.1 Schematic diagram of two dimension rectangular microchannel.

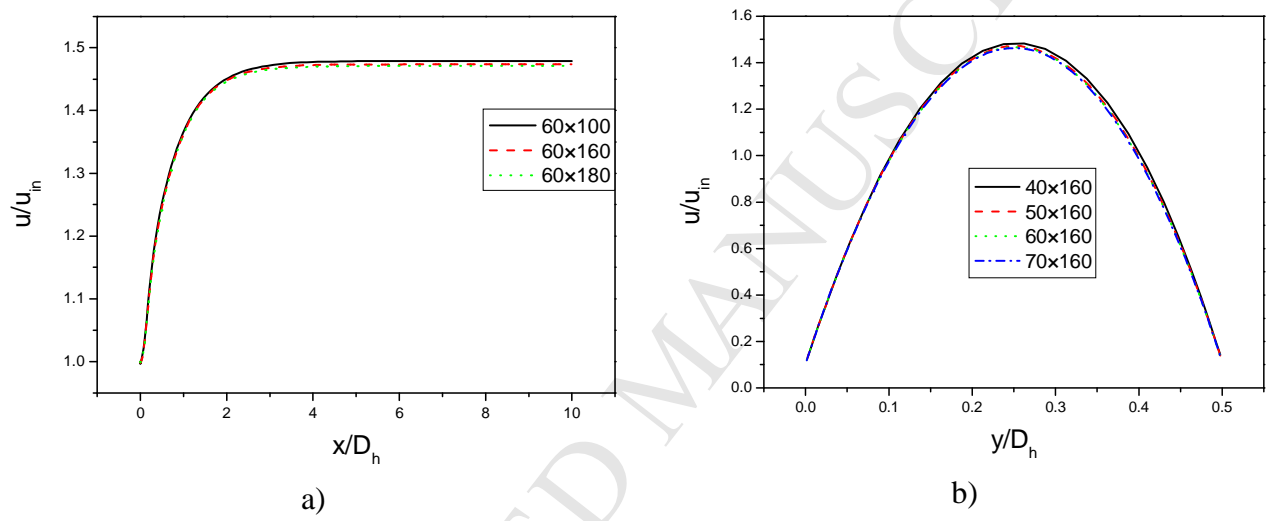


Fig.2 Grid independent test a) in x direction b) in y direction.

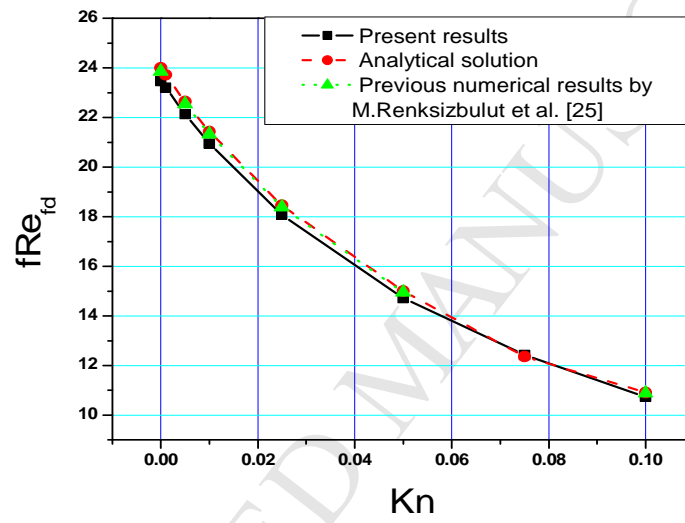


Fig.3 Compare the fully developed Poiseuille number with the previous numerical results by Renksizbulut et al. [25] and also with analytical results.

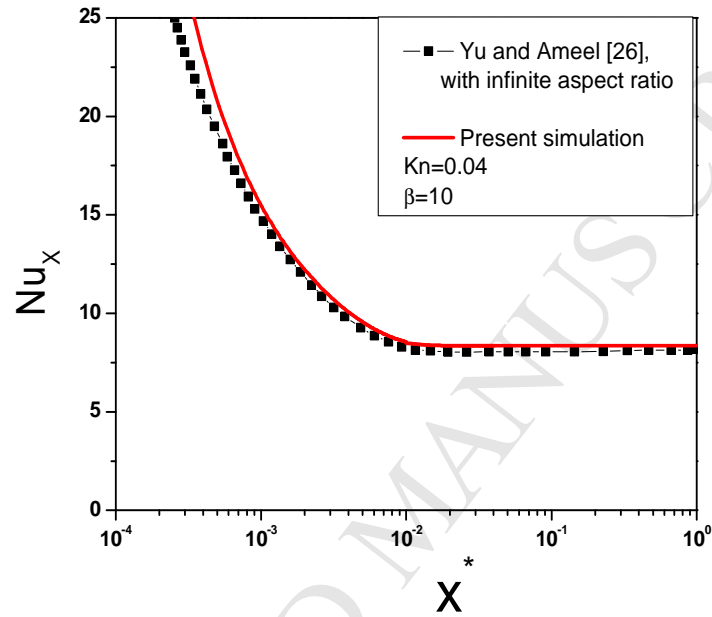


Fig.4 Compare the local Nusselt number with the previous numerical results by Yu and Ameer [26] for $Kn=0.04$ and $\beta=10$ with infinity aspect ratio.

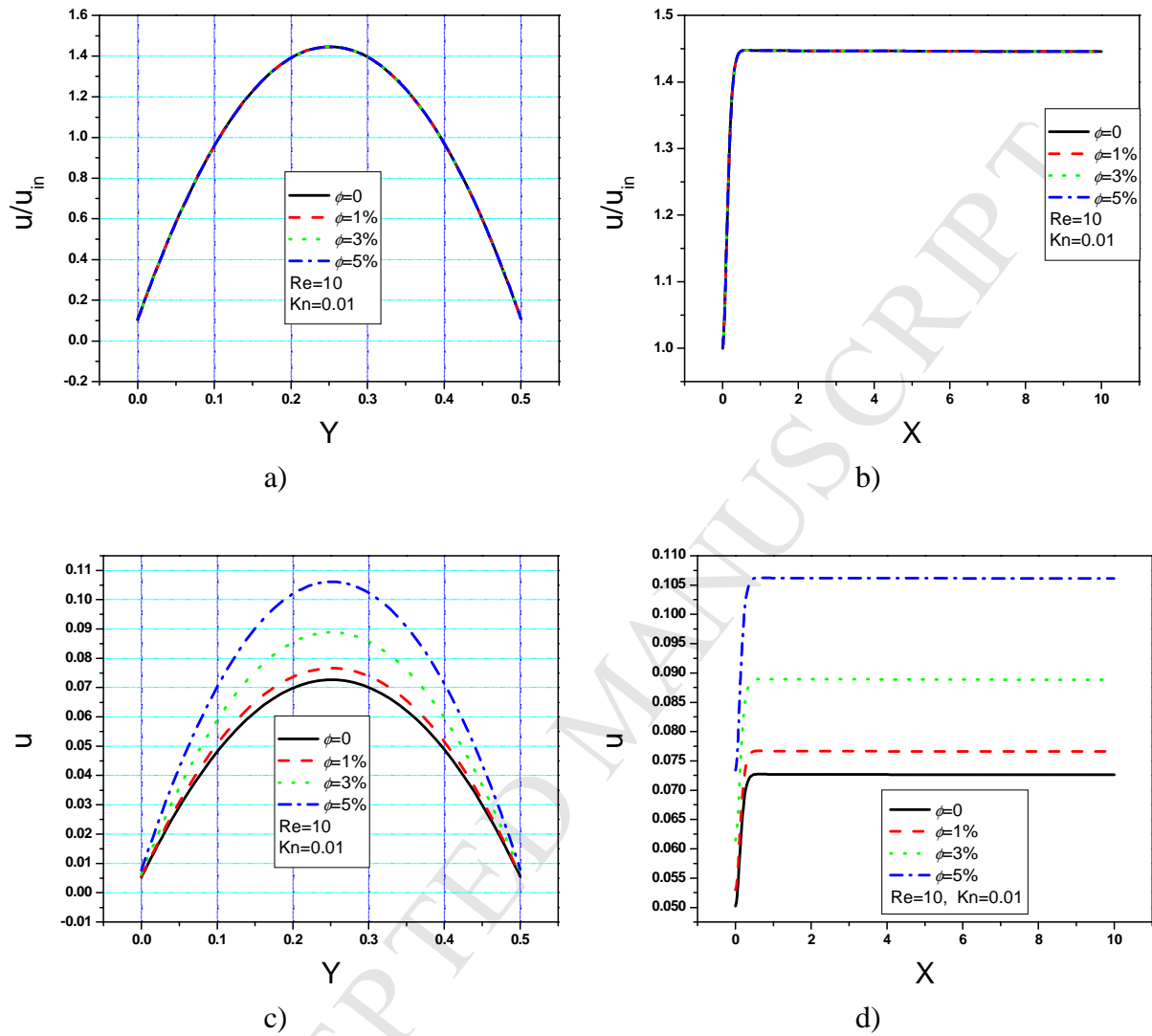


Fig.5 Variation of the non-dimensional velocity (a,b) and dimensional velocity profile (c,d) with nanoparticles concentration for $Re=10$ and $Kn=0.01$ at fully developed region a) and c), at centerline along the channel b) and d).

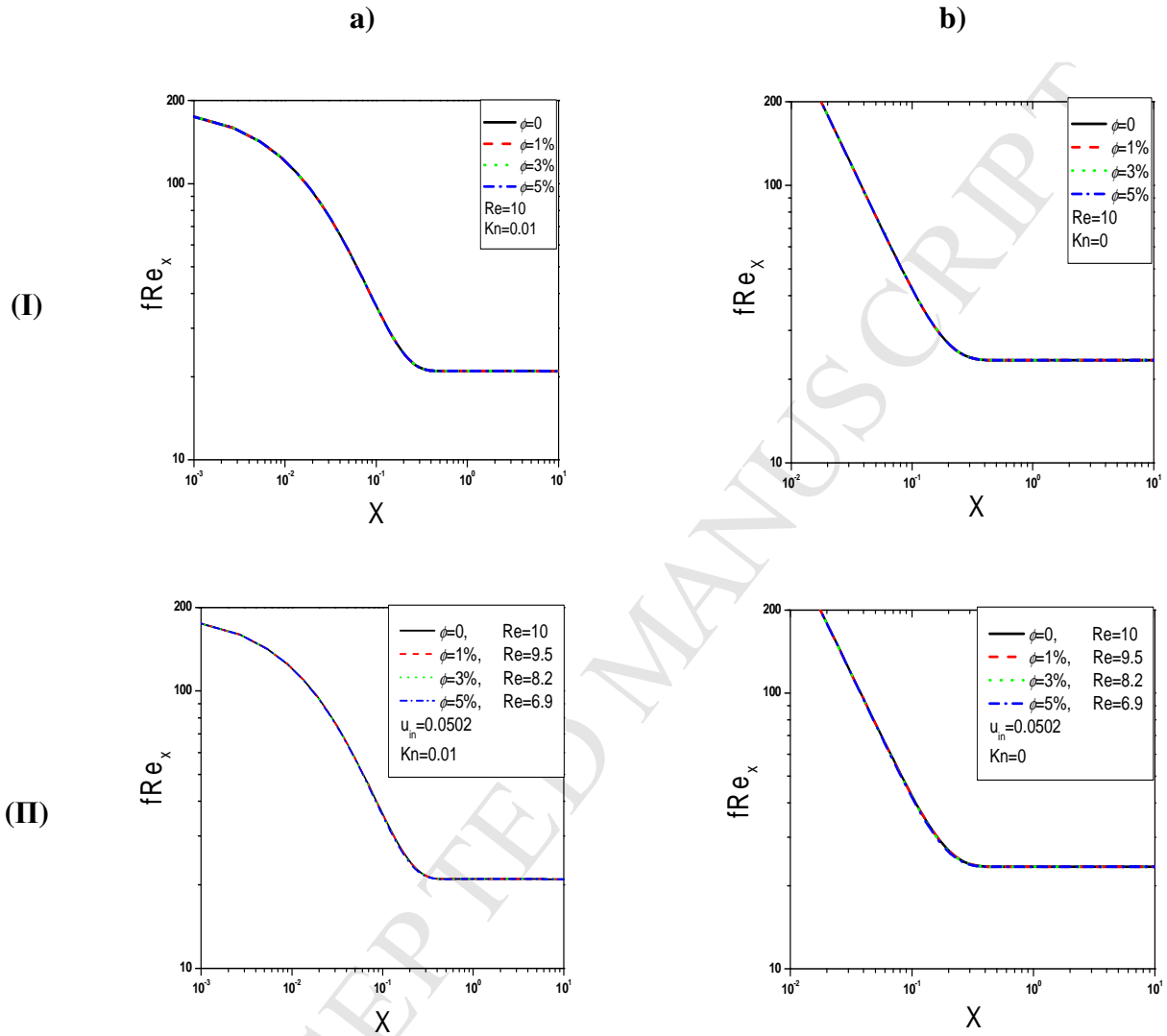


Fig.6 The local Poiseuille number profiles for first case (I) and second case (II) at $Re=10$ and different ϕ for a) slip flow regime ($Kn=0.01$) and b) non-slip flow regimes ($Kn=0$).

a)

b)

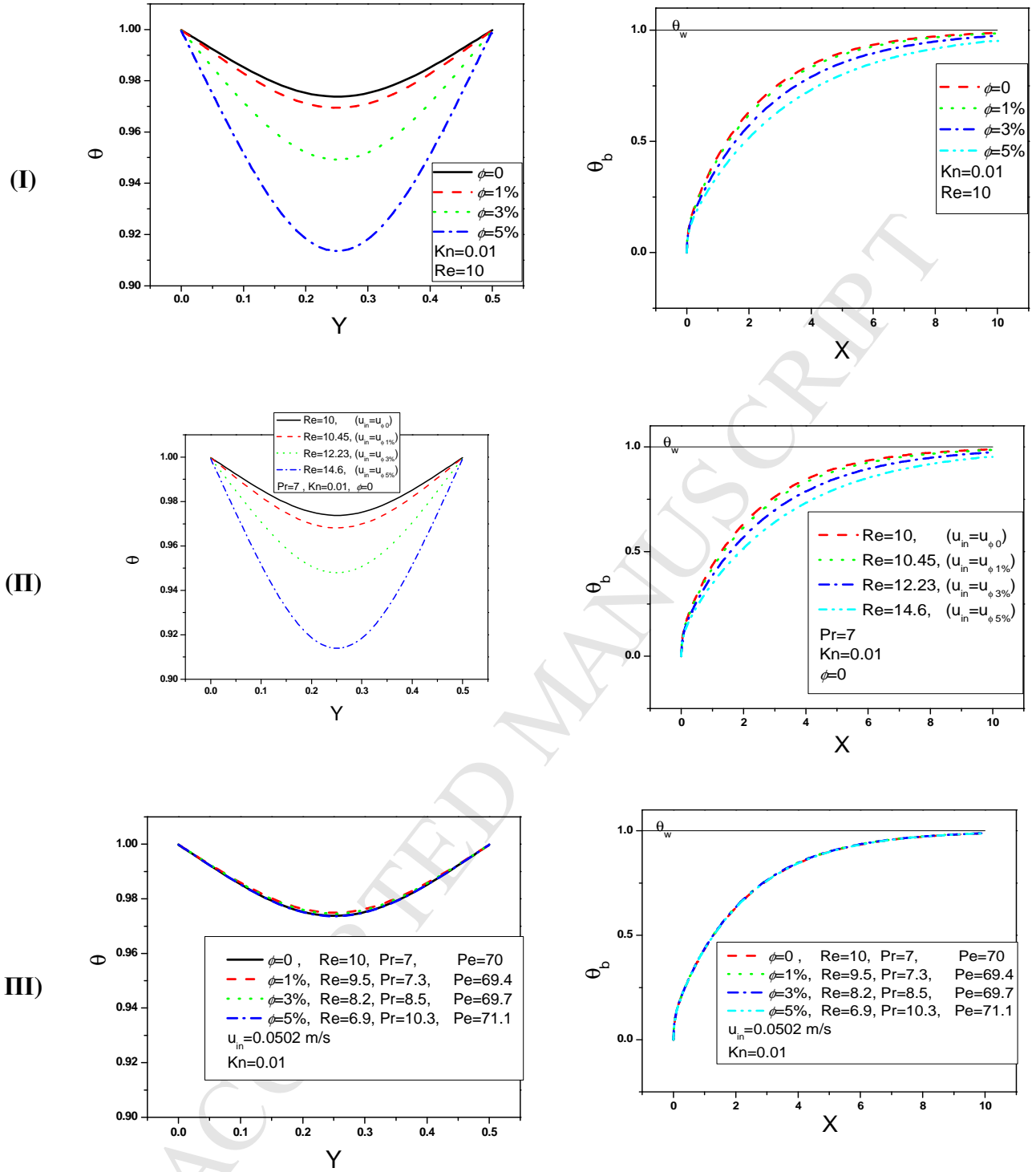


Fig.7 a) the non-dimensional temperature at the outlet and b) the non-dimensional bulk temperature profiles for first case (I), second case (II) and third case (III).

a)

b)

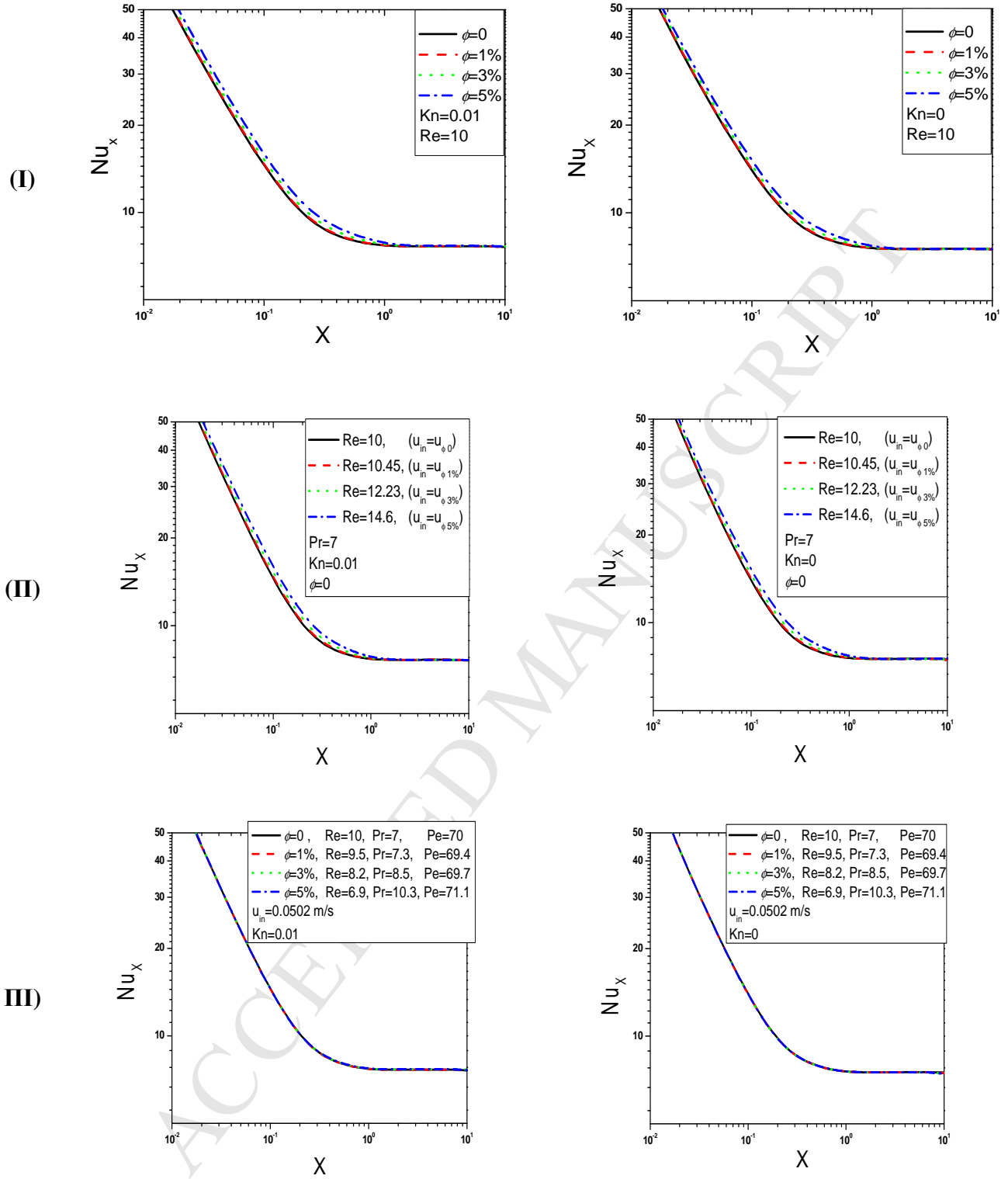


Fig.8 The local Nusselt number profiles for first case (I), second case (II) and third case (III)

for a) slip flow regime ($Kn=0.01$) and b) non-slip flow regimes ($Kn=0$).